A Simple Kinetic Model Describes the Processivity of Myosin-V

Anatoly B. Kolomeisky* and Michael E. Fisher[†]

*Department of Chemistry, Rice University, Houston, Texas 77005-1892; and [†]Institute for Physical Science and Technology, University of Maryland, College Park, Maryland 20742

ABSTRACT   Myosin-V is a motor protein responsible for organelle and vesicle transport in cells. Recent single-molecule experiments have shown that it is an efficient processive motor that walks along actin filaments taking steps of mean size close to 36 nm. A theoretical study of myosin-V motility is presented following an approach used successfully to analyze the dynamics of conventional kinesin but also taking some account of step-size variations. Much of the present experimental data for myosin-V can be well described by a two-state chemical kinetic model with three load-dependent rates. In addition, the analysis predicts the variation of the mean velocity and of the randomness—a quantitative measure of the stochastic deviations from uniform, constant-speed motion—with ATP concentration under both resisting and assisting loads, and indicates a *sub*step of size $d_0 \simeq$ 13 – 14 nm (from the ATP-binding state) that appears to accord with independent observations.

INTRODUCTION

Various classes of enzymes, usually termed motor proteins, play important roles in biological processes such as cellular transport, cell division, muscle function, and genetic transcription (see Lodish et al., 1995). What we may term translocatory motor proteins (in contrast to rotary motor proteins) are epitomized by kinesins, dyneins, myosins, and DNA and RNA polymerases that move under loads along polar linear tracks such as microtubules, actin filaments, and double-stranded DNA, the motion being fueled by the hydrolysis of ATP or related reactions.

Motor proteins may work collectively in large groups, like myosin in muscles, or they may operate individually as do most microtubule-based kinesin and dynein molecules (Leibler and Huse, 1993; Howard, 2001). Those motor proteins that function collectively are typically *non*processive, i.e., they make at most one mechanical step along their tracks during a catalytic cycle before detaching from the track. On the other hand, individual motors that move vesicles over long distances (up to several microns) need to stay bound to their tracks over many catalytic cycles: such motors are *processive*. For example, conventional kinesin motors can walk along microtubules taking a 100 or more 8.2-nm steps before dissociating (Howard et al., 1989; Block et al., 1990; Vale et al., 1996; Kojima et al., 1997).

Recently, single-molecule experiments by Mehta et al. (1999; Mehta, 2001), Rief et al. (2000), Sakamoto et al. (2000), Rock et al. (2001), Veigel et al. (2002), and Nishikawa et al. (2002) have demonstrated that myosin-V and myosin-VI, in contrast to the behavior of other members of the myosin superfamily (Howard, 2001), are also efficient

processive molecular motors. Here we will focus on the dynamics of myosin-V.

Myosin-V is a dimeric, two-headed molecule that in the presence of actin readily hydrolyzes ATP to produce ADP and P_i (Mehta, 2001). Kinetic experiments in bulk solution (De La Cruz et al., 1999, 2000; Mehta, 2001) have demonstrated that release of ADP is the rate-limiting step in the actin-activated ATPase cycle. Under conditions of limiting ATP the kinetically prevalent state appears to have both head domains bound to the actin filament as captured in electron micrographs by Walker et al. (2000); but, more generally, see the discussions in Mehta (2001) and De La Cruz et al. (2001).

Optical traps equipped with electronic feedback mechanisms have provided valuable information regarding the dynamics of individual myosin-V molecules under low load (see Mehta, 2001). The experiments allow one to monitor the displacement, $x(t)$, of a single molecule as a function of the time t under different concentrations of ATP, etc., while maintaining a steady external load, F, which opposes the directed motion of the motor.

The principle experimental findings can be summarized as follows: first, myosin-V moves along actin filaments toward the plus or barbed end, taking large steps of size averaging 35 – 38 nm (Mehta et al., 1999) approximating the 37-nm pseudo-repeat of the actin filament (Bray, 2001); second, the stepping dynamics depends strongly on the ATP concentration: thus, the mean dwell time $\tau(F, [\text{ATP}])$ observed between successive steps (preceding a forward step) at low [ATP] ($=1\ \mu$M) hardly varies with the external load, while under saturating conditions ([ATP] $\geq$ 2 mM) the mean dwell time grows rapidly as F approaches the stall force, $F_S = 3.0 \pm 0.3$ pN (at which, on average, the motor just fails to progress); third, the overall stepping rate or mean velocity,

$$V(F, [\text{ATP}]) \approx d\langle x(t)\rangle/dt, \qquad (1)$$

follows a Michaelis-Menten form in that it is proportional to [ATP] at low concentrations but becomes independent of [ATP] under saturating conditions; fourth, tight coupling

between chemical and mechanical cycles is valid, with one ATP molecule hydrolyzed per individual myosin-V forward step along an actin filament; but, fifth, in contrast to the dynamics of conventional kinesin (Coppin et al., 1997; Visscher et al., 1999), myosin-V under load not infrequently exhibits sequences of two or three reverse or backward steps; and, finally, the addition of ADP to the in vitro solution significantly reduces the turnover rate of ATP (as is to be expected); moreover, the inhibitory effect of ADP scales with the concentration of ATP (Rief et al., 2000) (and even when the mean stepping rate is reduced twofold, the distribution of dwell periods is unaltered).

The growing quantity of information concerning myosin-V has naturally stimulated theoretical discussions of the dynamics. Several models have been proposed and are reviewed by Mehta (2001). In particular, to provide an explanation of the observed load-dependence of the processivity, the mean dwell time at temperature T has been modeled phenomenologically (following a proposal of Wang et al., 1998) as a sum of two terms, namely

$$\tau(F) = \tau_1 + \tau_2 \exp(Fd'/k_\mathrm{B}T), \qquad (2)$$

corresponding, respectively, to putative force-independent and force-dependent transitions. It is natural to expect here that d' corresponds to the observed step size $d \simeq 36\,\mathrm{nm}$ (Fisher and Kolomeisky, 1999, 2001; Hille, 2001). However, fitting the experimental data of Mehta et al. (1999), which is displayed in Fig. 2 below, necessitates an (effective) step size d' of $10-15\,\mathrm{nm}$, which is only $30-40\%$ of the actual step size. This discrepancy is rationalized by asserting that d' is some "characteristic distance over which load affects the catalysis rate." Furthermore, this approach fails to account clearly for the observed stalling of the motors at $F_\mathrm{S} \simeq 3.0\,\mathrm{pN}$. Clearly, a more soundly based quantitative theory for processivity of myosin-V seems called for to satisfactorily describe the currently available data and to provide testable predictions. The present article aims to meet these requirements.

We present a theoretical analysis of the dynamics of myosin-V using simple, discrete-state stochastic models which have recently been developed and analyzed in detail by Kolomeisky and Widom (1998), Fisher and Kolomeisky (1999a,b, 2001, 2002) and Kolomeisky and Fisher (2000a,b). This approach has been used successfully in Fisher and Kolomeisky (2001) to analyze the extensive experimental data on the dynamics of single conventional kinesin molecules moving in vitro along microtubules obtained by Visscher et al. (1999) and Schnitzer et al. (2000). We will demonstrate that most of the currently available experimental data on the processivity of myosin-V can be well accounted for by the simplest ($N = 2$)-state model embodying a theoretical picture in satisfactory accord with other kinetic and structural experiments. Our treatment also provides specific predictions for as yet unexplored features of myosin-V dynamics that can be tested experi-

mentally and should uncover further details of the stepping mechanism.

THEORETICAL APPROACH

For completeness we first outline briefly the class of stochastic models used in our analysis and the explicit analytical results available for them. In the simplest periodic sequential kinetic model, illustrated schematically in Fig. 1, the protein motor is viewed as moving along a linear periodic track and binding at specific sites located at $x = ld$ ($l = 0$, ± 1, ± 2, $\cdots$) where d is a fixed step distance. In a first treatment of myosin-V on actin filaments we may adopt the observed mean value, $\bar{d} \simeq 36\,\mathrm{nm}$, corresponding to the helix repeat distance (Bray, 2001). However, as discussed further below, the analysis can be extended to take account of the variations in the individual step sizes seen in the data for myosin-V (Mehta et al., 1999; Rief et al., 2000; Walker et al., 2000; Veigel et al., 2002): the variation seems primarily to result from binding on actin monomers (at spacing 5.5 nm) adjacent to the main 6.5-monomer helix repeat distance (Steffen et al., 2001).

The basic model then supposes that in a catalytic cycle which translocates a motor from binding site l to $l + 1$ the protein undergoes N intermediate biochemical transitions from states $j_l = 0_l$ to 1_l to $2_l \cdots$ to $(N-1)_l$ to $N_l \equiv 0_{l+1}$. Kinetic rates u_j and w_j are associated with the transitions from state j_l forward to state $(j + 1)_l$ and backward to state $(j - 1)_l$, respectively. The state 0_l represents the motor tightly bound at site l in the absence of fuel molecules—ATP in the case of myosin-V. Binding of a fuel molecule is represented by the transition $0_l \rightarrow 1_l$, unbinding by $1_l \rightarrow 0_l$. Subsequent hydrolysis and release of products occur in the forward transitions $1_l \rightarrow 2_l \rightarrow \cdots$ But it is important to note that backward intermediate transitions and whole steps (possibly associated with reverse hydrolysis) are allowed and observed experimentally.

For this model, the mean velocity $V(\{u_j, w_j\})$ (see Eq. 1) may be expressed exactly in a closed analytic form in terms of the rate constants $\{u_j, w_j\}$ for any value of N (Fisher and Kolomeisky, 1999). Furthermore, similar explicit formulae
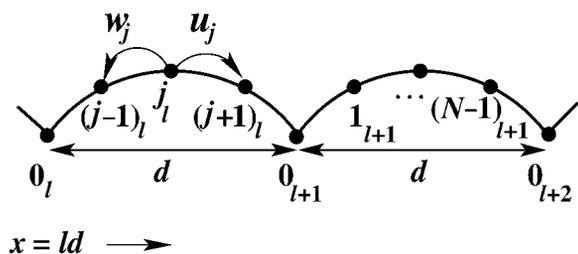

FIGURE 1 Specification of the simplest N-state periodic stochastic model. A motor in state j_l can undertake a forward transition at rate u_j or it can make a backward transition at rate w_j. The bound state N_l is identified with 0_{l+1}.

are available for the dispersion (or effective diffusion constant) of the motion, defined by

$$D = D(\{u_j, w_j\}) = \frac{1}{2} \lim_{x \to \infty} \frac{d}{dt} \left[\langle x^2(t) \rangle - \langle x(t) \rangle^2 \right]. \quad (3)$$

This measures the statistical deviation of the motor trajectories from uniform motion at constant velocity. The knowledge of both the velocity V and the dispersion D, conveniently combined in terms of *randomness* (Svoboda et al., 1994),

$$r = 2D/Vd, \quad (4)$$

serves to set bounds on N via a determination of the number of rate-limiting kinetic biochemical transitions and thus yields valuable information regarding the mechanism of processivity (Visscher et al., 1999; Kolomeisky and Fisher, 2000a; Fisher and Kolomeisky, 2001, 2002; Koza, 2002).

To account properly for the externally imposed force, F, it is essential (Fisher and Kolomeisky 1999, 2001) to introduce *load distribution factors*, θ_j^+ and θ_j^- (for $j = 0, 1, \ldots, N-1$). Then the transition rates may be taken to vary as

$$u_j \Rightarrow u_j(F) = u_j^0 \exp(-\theta_j^+ Fd/k_B T),$$
$$w_j \Rightarrow w_j(F) = w_j^0 \exp(\theta_j^- Fd/k_B T), \quad (5)$$

where the most reasonable requirement (Fisher and Kolomeisky, 1999, 2001; Hille, 2001) is

$$\sum_{j=0}^{N-1} (\theta_j^+ + \theta_j^-) = 1, \quad (6)$$

which implies that the condition of stall reflects stochastic quasiequilibrium among the (on-pathway) intermediate mechanochemical states. Indeed, these expressions embody a picture of load-dependent activation barriers for forward and reverse rates between intermediate states j that lie on a multidimensional reaction pathway. The load distribution factors $\theta_j^\pm$ provide significant mechanochemical information since they embody a projection of the valleys and cols (or passes) of the reaction pathway onto the force axis, which we suppose is parallel to the motor track. Thus, one may identify *substeps* of magnitude,

$$d_j = (\theta_j^+ + \theta_{j+1}^-)d, \quad (7)$$

between motor states j_l and $(j + 1)_l$. If the spatial fluctuations of the center of force of the motor in the intermediate states j_l and $(j + 1)_l$ are sufficiently small relative to d_j one may hope to identify this substep in suitably averaged traces $x(t)$ of individual motor motions (Fisher and Kolomeisky, 2002).

For the present purpose we note that the explicit expressions for the mean velocity, V, for general N lead to a simple relation for the stalling force as defined by $V(F \to F_S) \to 0$, namely,

$$F_S = \frac{k_B T}{d} \ln \left[\prod_{j=0}^{N-1} (u_j^0/w_j^0) \right]; \quad (8)$$

see Fisher and Kolomeisky (1999).

The N-state periodic kinetic model presented in Fig. 1 is, mathematically, an example of the general one-dimensional nearest-neighbor random hopping model for which first-passage questions have been much studied (see van Kampen, 1997). Of particular interest here are the so-called splitting probabilities and mean first-passage times. Specifically, to analyze observations of motor-protein dwell times, we need the ''single-step forward splitting probability,'' $\pi_+(\{u_j, w_j\})$, defined as the probability that a motor starting at site l will arrive at site $l + 1$ without having undergone sufficiently many intermediate reverse transitions to complete a full backward step from l to site $l - 1$. The corresponding conditional mean single-step first-passage time, $\tau_+(\{u_j, w_j\})$, then represents the average time a motor spends at site l before leaving and making a forward step to site $l + 1$. Because of the periodic structure of the N-state model of Fig. 1 the (rather elaborate) expressions developed by van Kampen (1997) can be simplified considerably even for general N (Kolomeisky and Fisher, unpublished). Here we quote the simplest $N = 2$ results which will suffice for our present purposes, namely, for the mean forward-step dwell time,

$$\tau_+ = (u_0 + u_1 + w_0 + w_1)/(u_0 u_1 + w_0 w_1), \quad (9)$$

whereas the fraction of backward (or reverse) steps is

$$\pi_- = 1 - \pi_+ = w_0 w_1/(u_0 u_1 + w_0 w_1). \quad (10)$$

Finally, we mention that the basic model exhibited in Fig. 1 can be extended in various ways while still retaining explicit expressions for V, D, etc. In particular, one may allow for detachments or ''death'' rates, δ_j, from the various motor states and for branching (Kolomeisky and Fisher, 2000a), for parallel site-to-site ''jumping'' (Kolomeisky and Fisher, 2000a), for parallel biochemical processes (Kolomeisky, 2001), and for waiting time distributions and the associated *degrees of mechanicity*, $M_j^\pm$, of the various intermediate processes (Fisher and Kolomeisky, 1999, 2001; Kolomeisky and Fisher, 2000b). However, the range of observational data so far obtained for myosin-V (unlike that known for kinesin) does not yet warrant consideration of these extensions.

ANALYSIS OF MYOSIN-V DATA

The bulk-solution kinetic data on myosin-V ATPase activity indicate that at least two processes, namely, ATP binding and ADP release, should be taken into account in analyzing the motility (De La Cruz et al., 1999; Mehta, 2001). While recognizing that a more complete description may require further intermediate states, it is appropriate, therefore to consider first the simplest ($N = 2$)-state model. Then, as indicated above, the states $j = 0$ correspond to a myosin-V molecule bound to the actin filament in the absence of ATP—presumably with both heads attached, one behind the other (Walker et al., 2000)—whereas $j = 1$ labels myosin-actin complexes with bound ADP. Thus, in the scheme advanced in Fig. 6 of Mehta (2001), the first and last

configurations correspond to $j = 0$, whereas the four intermediate states are gathered into $j = 1$; in Fig. 4 of Rief et al. (2000) the $j = 0$ state corresponds to that labeled V; in Fig. 9 of De La Cruz et al. (2001) the second configuration corresponds to $j = 0$; and the remaining three to $j = 1$.

It now follows that the forward ATP-binding rate should take the form $u_0^0 = k_0^0[\text{ATP}]$, where the superscripts 0 denote the limit of zero load: see Eq. 5. On the other hand, the reverse unbinding rate, w_1, and the forward, ADP release

the mean velocity simply via $\bar{\tau} = d/V$—although at low loads, where the fraction of reverse steps is small, $\bar{\tau}$ should provide a good approximation; but under near stall conditions, when $V \rightarrow 0$, the overall mean step time, $\bar{\tau}$, diverges to infinity whereas the dwell times $\tau(F \rightarrow F_S)$ remain bounded. Rather, we identify the observed dwell times with the conditional single-step mean first-passage times, τ_+, introduced above: see Eq. 9. Accordingly, our analysis of the myosin-V data is based upon the expression

$$\tau(F, [ATP]) = \frac{k_0^0[\text{ATP}]e^{-\theta_0^+ Fd/k_BT} + u_1^0 e^{-\theta_1^+ Fd/k_BT} + k_0'[\text{ATP}]e^{\theta_0^- Fd/k_BT} + w_1^0 e^{\theta_1^- Fd/k_BT}}{k_0^0[\text{ATP}]e^{-\theta_0^+ Fd/k_BT}u_1^0 e^{-\theta_1^+ Fd/k_BT} + k_0'[\text{ATP}]e^{\theta_1^- Fd/k_BT}w_1^0 e^{\theta_1^- Fd/k_BT}}, \quad (11)$$

rate, u_1, should be independent of [ATP], but, of course, may depend on F.

According to standard chemical kinetic arguments, the backward rate w_0 should, in principle, be proportional to [ADP]; and, indeed, the concentration of P_i should also play a role. Note, particularly, in this connection the high affinity of ADP for actomyosin which, as discussed by Mehta (2001) and De La Cruz et al. (2000), had led to significant discrepancies in estimates of steady-state cycling rates. The detailed measurements (Mehta et al., 1999; Rief et al., 2000) have, therefore, been performed with the aid of an ATP regeneration system (as previously adopted in the kinesin experiments of Visscher et al., 1999). In such a setup neither the concentration of ADP, nor that of P_i, is monitored. While experiments that do control [ADP] and [P_i] separately are much to be desired, in their absence we are forced (as in Kolomeisky and Fisher, 2001) to model the ATP regeneration scheme more or less phenomenologically. Thus if, first, we suppose $w_0^0 = k_0'[\text{ATP}]^\alpha$ (which amounts to [ADP] $\propto$ [ATP]$^\alpha$), second, recall that the stall force, F_S, is given by Eq. 8, and, lastly, note that the current experimental observations reveal no significant dependence of F_S on [ATP] (Mehta, 2001), we are led to adopt $\alpha = 1$. Indeed, in light of the use of ATP-regeneration in the experiments, the proportionality of [ADP], and hence of w_0, to [ATP] at low concentrations is to be expected: see also Fisher and Kolomeisky (2001). It should be remarked, however, that the details of our description of the ATP regeneration scheme play only a minor role in fitting the myosin-V processivity data.

Now in many previous experimental studies of processive motor proteins the mean velocities, $V([\text{ATP}], F)$, have been measured and reported. Such observations must, at least in principle, include some fraction of backward or reverse steps, especially at large loads approaching stall. However, in their experiments on myosin-V (Mehta et al., 1999; Rief et al., 2000) the authors opted to measure only dwell times, separating adjacent steps of mean size $d \simeq 36$ nm (Mehta, 2001), *preceding forward steps*. Thus their reported dwell times, $\tau([\text{ATP}], F)$, as plotted in Fig. 2 *A*, do *not* precisely correspond to an ''overall mean step time,'' say $\bar{\tau}$, related to

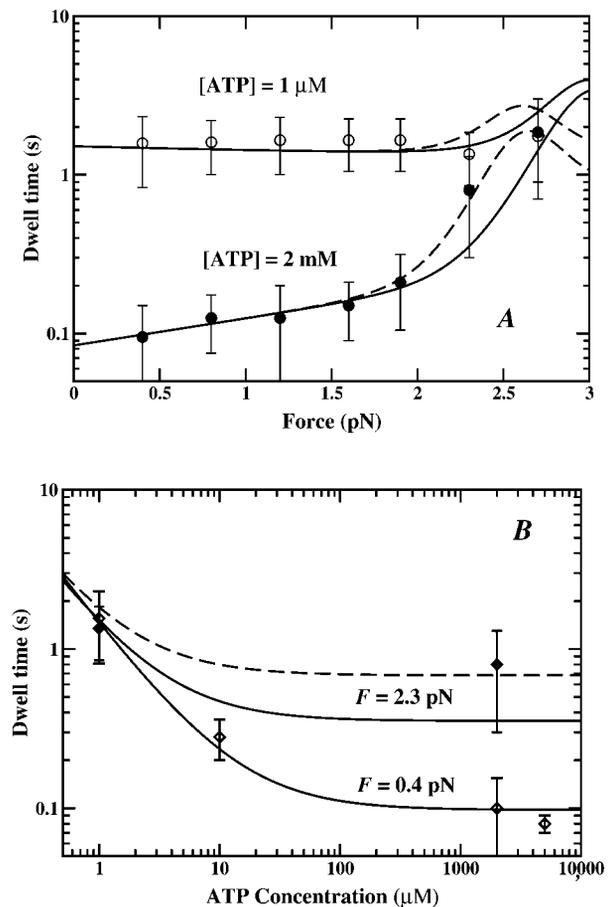following from Eqs. 5, 6, and 9, with $d = \bar{d} = 36$ nm.

FIGURE 2   Fits to the data of Mehta et al. (1999) for the mean dwell times of myosin-V: (*A*) as a function of external load, F, at different ATP concentrations; (*B*) as a function of [ATP] under an external load $F = 0.4$ pN and a prediction for $F = 2.3$ pN. The solid curves represent Eq. 11 with the central parameter values in Eqs. 12 and 13; the dashed curves represent the mean dwell times predicted for a 50:50 mixture of short, $d_{(-)} = 30.5$ nm, and long, $d_{(+)} = 41.5$ nm steps using the same values for the other parameters: see Variability of Step Sizes. (Note that in *B* the dashed curve for $F = 0.4$ pN cannot be distinguished from the solid curve.)

Then, by systematically exploring the full seven-dimensional parameter space specified by $(k_0^0, \cdots, \theta_0^-)$ we find that the observed stall force, F_S, and the dynamics of myosin-V as a function of [ATP] and of the load, F, up to F_S, are well described by the rates

$$k_0^0 = 0.70 \pm 0.10 \, \mu\text{M}^{-1}\text{s}^{-1}, \quad u_1^0 = 12.0 \pm 1.0 \, \text{s}^{-1}$$
$$k_0' = (5.0 \pm 0.5) \times 10^{-6} \, \mu\text{M}^{-1} \, \text{s}^{-1},$$
$$w_1^0 = (6.0 \pm 0.5) \times 10^{-6} \, \text{s}^{-1}, \tag{12}$$

and the load-distribution factors

$$\theta_0^+ = -0.010 \pm 0.010, \quad \theta_1^+ = 0.045 \pm 0.010,$$
$$\theta_0^- = 0.580 \pm 0.010, \quad \theta_1^- = 0.385 \pm 0.010. \tag{13}$$

It should be noted that consideration of the limits of low and high [ATP] and low and high loads confirm a fair degree of independence of the various fitting parameters. The uncertainties indicated in Eqs. 12 and 13 correspond to the ranges of acceptable fits to the processivity data while constraining the other parameters appropriately. The central values yield the fits presented in Fig. 2 as solid curves.

In respect to our fits for k_0^0 and u_1^0 note that the bulk solution kinetic experiments yield an ATP binding rate constant (corresponding to k_0^0) between 0.7 and 1.6 $\mu\text{M}^{-1} \, \text{s}^{-1}$, whereas the ADP-release rate (corresponding to u_1^0) is ~12–16 s^{-1} (Mehta, 2001; De La Cruz et al., 1999). The agreement is clearly most satisfactory.

DISCUSSION

Mean velocity and load dependence

The quality of the fits in Fig. 2 ensures that the observed (approximate) Michaelis-Menten behavior is respected. Indeed, using the rate and load-distribution parameters in Eqs. 12 and 13 and previous theory (e.g., Fisher and Kolomeisky, 2001) enables us to predict the variation of the mean velocity, V, with F and [ATP]: see the solid curves Fig. 3. Evidently, the stall force of ~3 pN seen in the experiments is reproduced. Note also, from the dwell-time data imposed on the predictions in Fig. 3 using $V \simeq d/\tau$, that, as anticipated in the discussion before Eq. 11, the approximation $\tau \simeq \bar{\tau} \equiv d/V$ is valid for small loads (up to $F \simeq 2.5$ pN). Indeed, from Eq. 10 (with Eqs. 5, 6, 12, and 13) one finds that the fraction of reverse steps is negligible until $F \gtrsim 2.5$ pN.

Load dependence of rates

It is notable from Eq. 13 that within the fitting uncertainties there is essentially no load-dependence to the binding of ATP to the myosin-V-actin complex, i.e., $\theta_0^+ \simeq 0$; see also Mehta (2001). This contrasts strongly with the properties of conventional kinesin moving on a microtubule where $\theta_0^+ \simeq 0.13$ was found in Fisher and Kolomeisky (2001) for both $N = 2$ and $N = 4$ fits. This lack of load-dependence on
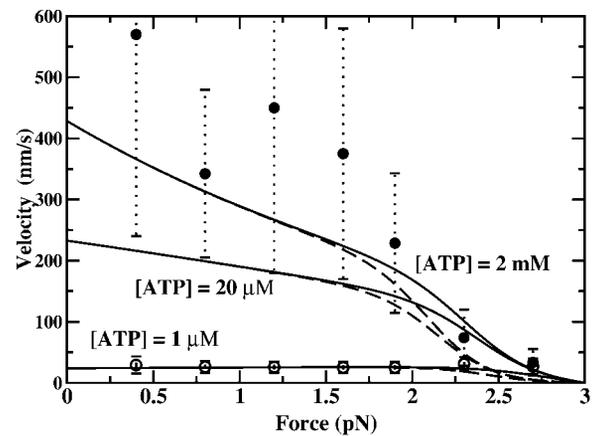

FIGURE 3 The force-velocity or (F, V) dependence of myosin-V at various concentrations of ATP as predicted using the parameter values in Eqs. 12 and 13: solid curves. The corresponding dashed curves follow from a model with alternating long and short steps ($d_{(+)} = 41.5$ nm and $d_{(-)} = 30.5$ nm) but otherwise the same zero-load rate constants and load distribution factors, $\theta_j^\pm$. The superimposed data bars (for [ATP] = 1 μM and 2 mM) derive from the observed dwell times by using the approximate relation $V \simeq d/\tau$ (with $d = 36$ nm); they track the predictions for $V(F)$ fairly well because of the paucity of reverse or backward steps under loads $F \lesssim 2.5$ pN.

binding ATP to actin-myosin accounts for the fact that the dwell time remains constant at saturating ATP conditions up to $F \simeq 2.3$ pN : see Fig. 2 A.

Nevertheless the other transitions are load-dependent with ADP release bearing a modest (~5%) fraction of the dependence. In parallel to kinesin, however—see Fisher and Kolomeisky (2001), the reverse transitions carry most of the load-dependence. Indeed, the load distribution pattern (Fisher and Kolomeisky, 2001) for myosin-V is close to a featureless descending ramp. Note that this result is in striking contrast to the implications of the phenomenological expression Eq. 1 which suggests that only forward (i.e., binding and/or hydrolysis) processes need be considered and could exhibit significant load-dependence. Indeed, our analysis indicates that at least three biochemical transitions in the actin-myosin-V ATPase cycle are load-dependent whereas Eq. 1 entails only a single load-dependent process. It seems that this difference is the main reason why fits for the "characteristic distance" d' in Eq. 1 differ so markedly from the true mean step size $\bar{d} \simeq 36$ nm. Since our analysis recognizes reverse transitions, which, by the fits, occur at a nonvanishing rate that is enhanced under load (see, again, Eq. 10), an explanation is provided for the observation of more frequent backward steps in myosin-V at high loads (Rief et al., 2000). Our treatment also provides a basis for a quantitative discussion of the ADP inhibition effect which it would be instructive to explore further experimentally.

Substeps

A striking feature of the data of Rief et al. (2000) is the observation of "half steps" under high loads ($\gtrsim 2$ pN).

From the published traces the steps appear to correspond to an intermediate state with a mean center of force lying a distance, say $d_{1/2}$ forward from the bound-state ($j = 0$) center with $d_{1/2}/d \simeq 0.48 \pm 0.04$. On the other hand, Eq. 7 and the load distribution factors in Eq. 13 indicate a substep with $d_0/d \simeq 0.38 \pm 0.03$ (corresponding to $d_0 \simeq 13 - 14$ nm). Rief et al. (2000) suggest that these half-steps (always followed by a complementary forward or backward step to complete a movement with $\langle \Delta x \rangle = d$ or 0) reflect an "off-pathway state," because they remain rare even under the high loads that uncover their presence. Although this suggestion seems most reasonable on the available evidence, our analysis suggests that the half-steps might possibly represent genuine substeps (lying on or close to the main reaction pathway), which appear stochastically under high loads when the forward rates, $u_1(F)$, have been slowed down whereas the reverse rates $w_1(F)$ are significantly enhanced.

In other experiments Veigel et al. (2002) observed attachments of single myosin-V molecules to an actin filament (stretched between two optically trapped beads) at [ATP] = 100 μM. After some of the attachment events, "staircases" of from two or three to a dozen forward steps were seen of mean size 36 nm; the staircases typically terminated in an effective stall (signaled by interspersed forward and backward steps) before detachment from the filament (see Fig. 3 of Veigel et al., 2002). However, the authors concluded that the *first step* in each staircase had a mean size of only $d_1 = 26.2 \pm 2.3$ nm (similar to the amplitude of isolated attachment events lacking any subsequent steps). A similar initial unitary step of $\sim$20 nm was seen in experiments by Moore et al. (2001) on heavy meromyosin-like fragments of myosin-V. These displacements were identified (in both articles) as a "working stroke," and Veigel et al. (2002) saw a comparable step of $\sim$21 nm in attachment events of a single-headed recombinant myosin-V. Furthermore, Veigel et al. (2002) in their Fig. 5 *A*, report stiffness measurements (using a sinusoidal driving force) which revealed low-stiffness intervals of variable durations (longer at higher loads): the midpositions of these intervals was $\sim$20 nm further along the actin filament than the preceding higher-stiffness intervals, a displacement similar to the initial "working stroke."

In our formulation and fits using a single intermediate mechanochemical state before completion of a full ($d = 36$ nm) step, such a d_1 should, as the notation chosen suggests, correspond to a $d - d_0 \simeq 22$ nm substep. The agreement of these various findings (within the combined experimental and fitting uncertainties) appears to lend support to our values for the load-distribution factors $\theta_j^{\pm}$. However, corresponding substeps have not been identified at low loads by Mehta, Rief, and co-workers. Nevertheless, a detailed examination of the sample stepping records for [ATP] = 2 mM and $F = 1$ pN presented in Fig. 2 *A* of Rief et al. (2000) reveals plausible indications of substeps in 13 to 16 of a total of $\sim$32 full steps of 36 nm, some of the substeps

appearing to have dwell times as long as $0.1 - 0.2$ s. More favorable conditions for detecting the predicted substeps and checking their dwell times should be realized at low loads and [ATP] 10 μM (which corresponds roughly to the effective Michaelis-Menten concentration, K_M; see Rief et al., 2000, and Fig. 3). Such data not consistent with the present predictions might require the introduction of waiting-time distributions (Kolomeisky and Fisher, 2000b): see also the remarks below concerning randomness.

Variability of step sizes

The fits to the data so far described have utilized a fixed step size, d, taken equal to the observed mean step size $\bar{d} \simeq 36$ nm that corresponds closely, as mentioned above, to the known (half) repeat distance of the actin filament double helix (Bray, 2001). But separate single-molecule experiments by Steffen et al. (2001) using myosin-S1 motor domains indicate "target zones" for binding to the filament consisting of three adjacent accessible actin monomers at spacings $\Delta d \simeq 5.5$ nm, the active zones repeating along the filament helices at $\sim$36-nm intervals. Furthermore, the processivity data for myosin-V reveal significant variations in individual step sizes about the mean, $\bar{d}$. The observations (see Mehta et al., 1999, Table 1; Rief et al., 2000, Fig. 2 *B*; Walker et al., 2000, Fig. 2; Veigel et al., 2002, Fig. 3 *b*) are consistent with $\sim$60% of the steps being of size $d_{(0)} = 36$ nm whereas 20% each are of sizes $d_{(\pm)} = d_{(0)} \pm \Delta d = 41.5$ and 30.5 nm; only a few percent of longer or shorter steps appear. The fact that $40 - 45\%$ of the observed steps deviate from $d_{(0)} = 36$ nm raises the possibility that our fits using a unitary step size might be misleading or especially sensitive to the spread in sizes.

To address this issue note, first, that steps of distinct sizes, say $d_{(k)}$, should be expected to have different mean dwell times: an ideal set of experimental observations would, then, report the corresponding $\tau_{(k)}(F,[\text{ATP}])$ and their probabilities, say p_k. An analysis using Eq. 11 with d replaced by $d_{(k)}$, etc., could subsequently be performed for each set and might possibly prove revealing. To a leading approximation one may suppose the various dwell times will be independent: in that case, the overall mean dwell time should be given by

$$\tau = \sum_k p_k \tau_{(k)}. \qquad (14)$$

More realistically, however, if the target-zone picture is valid, there will be correlations between successive steps: thus on average a short step, say of size $d_{(-)}$, must be followed immediately by a longer step, of size $d_{(0)}$ or $d_{(+)}$, and vice-versa. In principle, such correlations are open to observation and one might, indeed, expect the dwell times to depend on the size of the *previous* step, say $d'_{(k)}$, as well as on the step to be made. Theoretically the situation could clearly be modeled by a Markov process (see Steffen et al., 2001).

In the absence of such more detailed observations, however, we may test the sensitivity of our fits by further exploratory calculations. As an extreme case, suppose 50% of the steps are of magnitude $d_{(+)} = 41.5$ nm and 50% of size $d_{(-)} = 30.5$ nm. How would the fits change from those assuming a unitary step $d_{(0)} = 36$ nm? An answer is displayed by the dashed curves plotted in Fig. 2. These have been obtained by using Eq. 14 with $p_+ = p_- = 1/2$ and computing $\tau_{(+)}$ and $\tau_{(-)}$ from Eq. 11 using $d_{(+)}$ and $d_{(-)}$ together with the same zero-load rates and load distribution factors given in Eqs. 12 and 13. As evident from Fig. 2, there is no significant change in the quality of the fits—even though it would not be unreasonable to suppose that the rates and load factors might have some dependence on the $\pm 15\%$ changes in step-size. One might say that "the averages win out"—a not unexpected conclusion.

In fact we may go further and study the effects of *correlated step sizes* by utilizing the expressions for N-state periodic models (Kolomeisky and Fisher, 2000) with N an integral multiple of N_0, the number of intermediate states in the basic catalytic cycle. In our analysis we have $N_0 = 2$ and so can utilize an $N = 2 + 2 = 4$ periodic system to describe *alternating long and short steps* of sizes $d_{(+)}$ and $d_{(-)}$ (with, of course, the same previous *average* step size $d_{(0)}$). If we again use the zero-load rates and distribution factors in Eqs. 12 and 13, and compute the mean velocity as a function of load, we obtain the dashed curves presented in Fig. 3. Once more the deviations from the $d = \bar{d}$ results are negligible at loads $F < 2$ pN, whereas at higher loads sufficiently precise data might reveal discrepancies.

We conclude, therefore, that the consequences of replacing a distribution of step sizes by the mean $\bar{d}$ are not significant at current levels of experimental precision. Conversely, unless fairly precise experimental data can be obtained that are categorized by step length, there may be little more that can be reliably determined by fitting such observations.

Randomness

As mentioned previously, the fluctuation statistics of motor motion are effectively captured in the randomness parameter, r, as defined in Eq. 4. The fits presented in Eqs. 12 and 13 suffice to predict the variation of r with [ATP] under various loads (or vice versa) assuming that all the rate processes may be adequately represented as standard kinetic transitions: see Fisher and Kolomeisky (1999) and Kolomeisky and Fisher (2000). The corresponding predictions for $r([\text{ATP}])$ are presented in Fig. 4 for loads $F = 0.4$ and 2.5 pN. At low [ATP] the randomness is close to unity, indicating that only one rate-limiting process is effective in this concentration range. However, under a low load a marked dip to $r \simeq 0.5$ occurs around [ATP] $= 10–20$ μM: this, in turn, is indicative of two competing rate processes that both play a role in this "crossover" regime. On the other hand, at high
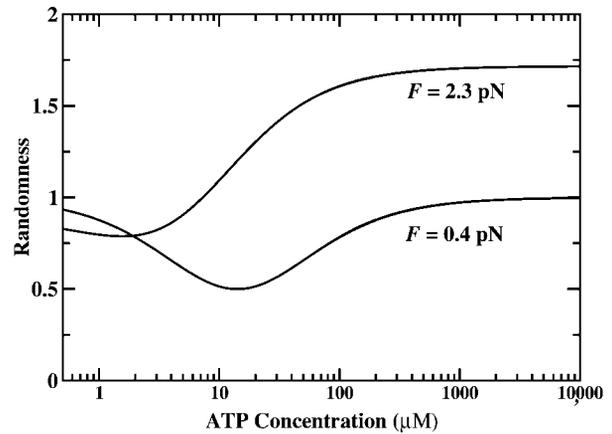

FIGURE 4 Predictions for the variation of the randomness, r, of myosin-V as a function of [ATP] at low ($F = 0.4$ pN) and high external load ($F = 2.3$ pN).

loads that approach stall, r rises rapidly above unity; however, this is primarily a consequence of the vanishing of the velocity V when $F \rightarrow F_S$ inasmuch as r must then diverge: see also Fig. 5 B, below.

It must be noted, however, that the analogous predictions, on the basis of an ($N = 2$)-state kinetic model, for the randomness of kinesin are not supported by the data of Visscher et al. (1999). Rather, for low loads and [ATP] $\gtrsim 30$ μM, the randomness falls rapidly and remains *below* 0.5 up to saturation concentrations: because of the bound $r \geq 1/N$ (Fisher and Kolomeisky, 1999; Koza, 2002), this is inconsistent with a kinetic description. Thus the data for conventional kinesin demand $N = 4$ (or more) states, in accord with the usual biochemical picture of ATP hydrolysis. *Alternatively*, and, in light of certain experiments (Nishiyama et al., 2001), possibly more realistically, one may invoke a waiting-time distribution to describe the process of hydrolysis and ADP release with a *mechanicity* $M_1 \simeq 0.6$ (Kolomeisky and Fisher, 2000; Fisher and Kolomeisky, 2001). Thus measurements of $r(F, [\text{ATP}])$ for myosin-V might well prove equally revealing of the mechanism by *failing* to verify the behavior predicted by Fig. 4.

Reverse or assisting loads

Another interesting and potentially instructive set of predictions can be advanced for the behavior under negative or assisting loads, $F < 0$. Such experiments have been performed for kinesin by Coppin et al. (1997). Although their data posed certain problems (in particular, a significantly lower overall processivity under low loads) the same load distribution factors (and similar rates) provided a not unreasonable ($N = 2$) fit (Fisher and Kolomeisky, 2001) simply by extending the analog of Eq. 11 to negative values of F. The corresponding predictions for myosin-V, for the dwell time and for the randomness as a function of F, extending down to -3 pN, are displayed in Fig. 5.
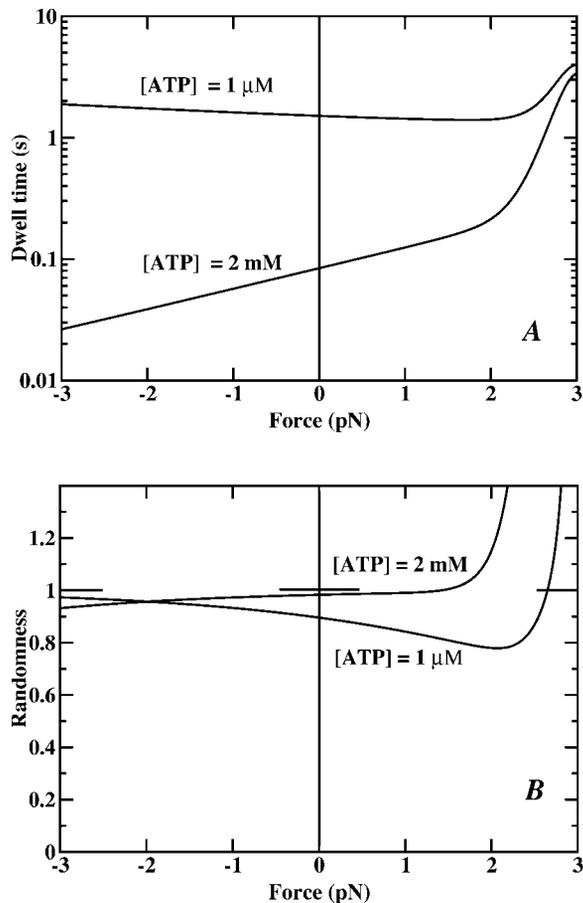
FIGURE 5 Predicted behavior of myosin-V under assisting (i.e., negative) and resisting (positive) external loads, F, for two ATP concentrations: (A) mean dwell time; (B) randomness. See the text for appropriate caveats.

A caveat must, however, again be raised in light of subsequent experiments on kinesin by Block (2001) and coworkers (Block et al., 2003; Lang et al., 2002). The validity of the extension of Eq. 11 to negative F clearly rests on a mechanistic/geometric assumption, namely, that changing abruptly the direction at which the coiled-coil myosin tail leaves the junction with two heads (or motor domains), i.e., from trailing upwards and backward ($F > 0$) to pulling upwards and forward ($F < 0$) does not result in a corresponding abrupt change in the mechanics of ATP binding, unbinding, or hydrolysis. If the junction were a perfect universal swivel joint, then as F (which is just the component of the total load force, say $\vec{F}$, parallel to the track), passes through zero, the stresses and strains within motor should, indeed, vary smoothly. However, the junction cannot be totally torsion free and if, for example, the tail were to rest against part of the head in one configuration but become dissociated in the other, then the smoothness assumption embodied in Eq. 5 would fail. Indeed, a fairly abrupt change of behavior has since been found by Block

et al. (2003) for kinesin. Clearly, comparable experiments on myosin-V are desirable and should prove informative.

CONCLUSIONS

In summary, we have presented a simple two-state stochastic model, with allowance for fluctuating step sizes, which describes well essentially all the available experimental data on single-molecule myosin-V processivity. It reveals that ATP binding is load-independent, whereas ADP release is weakly load-dependent, but (as for kinesin) the loading forces strongly affect the reverse transition rates. Our analysis is consistent with the observation of tight coupling between catalytic cycles and mechanical steps, i.e., one ATP molecule is consumed per individual step, and with ATP binding and ADP release rates measured in bulk solution. It also indicates that an intermediate myosin-ADP-actin complex has its center of force advanced by 13–14 nm forward from the position before ATP binding, in reasonable agreement with various observations indicating a subsequent "working stroke" of ~22 nm. We have discussed specific predictions for the dwell times, mean velocity, and randomness of myosin-V motors in various experimental regimes including the imposition of assisting loads. Further experiments are needed to investigate the validity of our theoretical description and to uncover other mechanochemical features of myosin-V.

REFERENCES

Block, S. M., L. S. B. Goldstein, and B. J. Schnapp. 1990. Bead movements by single kinesin molecules studied with optical tweezers. *Nature.* 348:348–352.

Block, S. M. 2001. Molecular Motors (Lecture). 55th Annual Meeting of the Society of General Physiologists, Sept. 9, 2001, Woods Hole, Massachusetts.

Block, S. M., C. L. Asbury, J. W. Shaevitz, and M. J. Lang. 2003. Probing the kinesin reaction cycle with a two-dimensional optical force clamp. *Proc. Natl. Acad. Sci. USA* [In press]

Bray, D. 2001. Cell Movements: From Molecules to Motility, 2nd Ed. Garland Publishing, New York. Chapter 5.

Coppin, C. M., D. W. Pierce, L. Hsu, and R. D. Vale. 1997. The load dependence of kinesin's mechanical cycle. *Proc. Natl. Acad. Sci. USA.* 94:8539–8544.

De La Cruz, E. M., A. L. Wells, S. R. Rosenfeld, E. M. Ostap, and H. L. Sweeney. 1999. The kinetic mechanism of myosin V. *Proc. Natl. Acad. Sci. USA.* 96:13726–13731.

De La Cruz, E. M., H. L. Sweeney, and E. M. Ostap. 2000. ADP inhibition of myosin V ATPase activity. *Biophys. J.* 79:1524–1529.

De La Cruz, E. M., E. M. Ostap, and H. L. Sweeney. 2001. Kinetic mechanism and regulation of myosin VI. *J. Biol. Chem.* 276:32373–32381.

Fisher, M. E., and A. B. Kolomeisky. 1999a. The force exerted by a molecular motor. *Proc. Natl. Acad. Sci. USA*. 96:6597–6602.

Fisher, M. E., and A. B. Kolomeisky. 1999b. Molecular motors and the forces they exert. *Physica A*. 274:241–266.

Fisher, M. E., and A. B. Kolomeisky. 2001. Simple mechanochemistry describes the dynamics of kinesin molecules. *Proc. Natl. Acad. Sci. USA*. 98:7748–7753.

Fisher, M. E., and A. B. Kolomeisky. 2002. The motion of kinesin on a microtubule. *Biophys. J.* 82:62a.

Hille, B. 2001. Ion Channels of Excitable Membranes. 3rd Ed. Sinauer Associates, Sunderland, Massachusetts. pp. 478–485.

Howard, J., A. J. Hudspeth, and R. D. Vale. 1989. Movements of microtubules by single kinesin molecules. *Nature*. 342:154–158.

Howard, J. 2001. Mechanics of Motor Proteins and the Cytoskeleton. Sinauer Associates, Sunderland, Massachusetts.

Kojima, H., E. Muto, H. Higuchi, and T. Yanagida. 1997. Mechanics of single kinesin molecules measured by optical trapping nanometry. *Biophys. J.* 73:2012–2022.

Kolomeisky, A. B. 2001. Exact results for parallel-chain kinetic models of biological transport. *J. Chem. Phys.* 115:7253–7259.

Kolomeisky, A. B., and B. Widom. 1998. A simplified ratchet model of molecular motors. *J. Stat. Phys.* 93:633–645.

Kolomeisky, A. B., and M. E. Fisher. 2000a. Periodic sequential kinetic models with jumping, branching and deaths. *Physica A*. 279:1–20.

Kolomeisky, A. B., and M. E. Fisher. 2000b. Extended kinetic models with waiting-time distributions: exact results. *J. Chem. Phys.* 113:10867–10877.

Koza, Z. 2002. Maximal force exerted by a molecular motor. *Phys. Rev. E.* 65:031905:1–5.

Lang, M. J., C. L. Asbury, J. W. Shaevitz, and S. M. Block. 2002. An automated two-dimensional force clamp for single molecule studies. *Biophys. J.* 83: 491–501.

Leibler, S., and D. A. Huse. 1993. Porters versus rowers: a unified stochastic model of motor proteins. *J. Cell Biol.* 121:1357–1368.

Lodish, H., A. Berk, S. L. Zipursky, and P. Matsudaira. 1995. Molecular Cell Biology, 3rd Ed. Scientific American Books, New York.

Mehta, A. 2001. Myosin learns to walk. *J. Cell Sci.* 114:1981–1998.

Mehta, A. D., R. S. Rock, M. Rief, J. A. Spudich, M. S. Mooseker, and R. E. Cheney. 1999. Myosin-V is a processive actin-based motor. *Nature*. 400:590–593.

Moore, J. R., E. B. Krementsova, K. M. Trybus, and D. M. Warshaw. 2001. Myosin V exhibits a high duty cycle and large unitary displacement. *J. Cell Biol.* 155:625–635.

Nishikawa, S., K. Homma, Y. Komori, M. Iwaki, T. Wazawa, A. H. Iwane, J. Saito, R. Ikebe, E. Katayama, T. Yanagida, and M. Ikebe. 2002. Class VI myosin moves processively along actin filaments backward with large steps. *Biochem. Biophys. Res. Commun.* 290:311–317.

Nishiyama, M., E. Muto, Y. Inoue, T. Yanagida, and H. Higuchi. 2001. Substeps within the 8-nm step of the ATPase cycle of single kinesin molecules. *Nature Cell Bio.* 3:425–428.

Rief, M., R. S. Rock, A. D. Mehta, M. S. Mooseker, R. E. Cheney, and J. A. Spudich. 2000. Myosin-V stepping kinetics: a molecular model for processivity. *Proc. Natl. Acad. Sci. USA*. 97:9482–9486.

Rock, R. S., S. E. Rice, A. L. Wells, T. J. Purcell, J. A. Spudich, and H. L. Sweeney. 2001. Myosin-VI is a processive motor with a large step size. *Proc. Natl. Acad. Sci. USA*. 98:13655–13659.

Sakamoto, T., I. Amitani, E. Yokota, and T. Ando. 2000. Direct observation of processive movement by individual myosin V molecules. *Biochem. Biophys. Res. Commun.* 272:586–590.

Schnitzer, M. J., K. Visscher, and S. M. Block. 2000. Force production by single kinesin motors. *Nat. Cell Biol.* 2:718–723.

Steffen, W., D. Smith, R. Simmons, and J. Sleep. 2001. Mapping the actin filament with myosin. *Proc. Natl. Acad. Sci. USA*. 98:14949–14954.

Svoboda, K., P. P. Mitra, and S. M. Block. 1994. Fluctuation analysis of motor protein movement and single enzyme kinetics. *Proc. Natl. Acad. Sci. USA*. 91:11782–11786.

Vale, R. D., T. Funatsu, D. W. Pierce, L. Romberg, Y. Harada, and T. Yanagida. 1996. Direct observation of single kinesin molecules moving along microtubules by fluorescence microscopy. *Nature*. 380:451–453.

van Kampen, N. G. 1997. Stochastic Processes in Physics and Chemistry, 2nd Ed. Elsevier, Amsterdam, The Netherlands. Chapter 12.

Veigel, C., F. Wang, M. L. Bartoo, J. R. Sellers, and J. E. Molloy. 2002. The gated gait of the processive molecular motor, myosin V. *Nat. Cell Biol.* 4:59–65.

Visscher, K., M. J. Schnitzer, and S. M. Block. 1999. Single kinesin molecules studied with a molecular force clamp. *Nature*. 400:184–189.

Walker, M. L., S. A. Burgess, J. R. Sellers, F. Wang, J. A. Hammer III, J. Trinick, and P. J. Knight. 2000. Two-headed binding of a processive myosin to F-actin. *Nature*. 405:804–807.

Wang, M. D., M. J. Schnitzer, H. Yin, R. Landick, J. Gelles, and S. M. Block. 1998. Force and velocity measured for single molecules of RNA polymerase. *Science*. 282:902–907.